Journal of Geophysical Research - Atmospheres

Supporting Information for

An intercomparison and validation of satellite-based surface radiative energy flux estimates over the Arctic

Aku Riihelä[1], Jeffrey R. Key[2], Jan Fokke Meirink[3], Peter Kuipers Munneke[4], Timo Palo[5], Karl-Göran Karlsson[6]

[1]Finnish Meteorological Institute (FMI), Erik Palménin aukio 1, FI-00560 Helsinki, Finland. Email: aku.riihela@fmi.fi

[2]National Oceanic and Atmospheric Administration (NOAA), 1225 West Dayton Street, Madison, WI 53706, USA, Email: jeff.key@noaa.gov

[3]Royal Netherlands Meteorological Institute (KNMI), Utrechtseweg 297, 3731 GA De Bilt, The Netherlands, Email: meirink@knmi.nl

[4]Institute for Marine and Atmospheric research, Utrecht University, PO Box 80.005, 3508 TA Utrecht, The Netherlands. Email: p.kuipersmunneke@uu.nl

[5]University of Tartu, Ülikooli 18, 50090 Tartu, Estonia. Email: timo.palo@ut.ee

[6]Swedish Meteorological and Hydrological Institute, Folkborgsvägen 17, SE-60176, Sweden. Email: Karl-Goran.Karlsson@smhi.se

Contents of this file

Text S1 – APP-x algoritm description.

Of particular interest in this study are surface albedo, surface temperature, and cloud optical depth. The clear-sky surface temperature algorithm uses a regression model to correct for atmospheric attenuation, much like those used for sea surface temperature estimation. To determine the empirical relationship, radiosonde data from drifting ice and land stations in the Arctic and Antarctic were used with a radiative transfer model to simulate the sensor brightness temperatures. Validation studies with in situ data show a bias of 0.2 K and a root-mean-square error (RMSE) of 1.9 K.

The retrieval of surface albedo involves four steps: AVHRR channels 1 and 2 reflectances are converted to a broadband reflectance, the top-of-atmosphere (TOA) broadband reflectance is corrected for anisotropy, the TOA broadband albedo is converted to a surface broadband albedo, and the surface clear sky broadband albedo is adjusted for the effects of cloud cover in cloudy pixels (Key et al. 2001). Validation studies with in situ data show a bias of -0.05 (absolute) and a root-mean-square error (RMSE) of 0.1.

Cloud optical depth is estimated using a comprehensive database (lookup table) of modeled reflectances and brightness temperatures covering a broad range of surface and atmospheric conditions. The approach for daytime retrievals follows that of Nakajima and King (1990), with simulations of reflectances and brightness temperatures done for a snow surface and high-latitude conditions. APP-x cloud optical depth has not been validated.

Text S2 – CLARA-A2 cloud properties description.

The CLARA-A2 cloud mask (yielding cloud cover CFC after aggregation) and thermodynamic phase (CPH) are based on multi-spectral threshold tests. Cloud-top temperature (CTT) is derived using two different radiance matching methods, one for clouds identified as opaque and one for semi-transparent clouds. Cloud optical thickness (COT) and particle effective radius (REFF) for the assigned phase are retrieved with the Nakajima-King method using AVHRR channels 1 (0.6 micron) and either 3a (1.6 micron) or 3b (3.7 micron). Since the retrieval of COT and REFF relies on reflected sunlight, these parameters are only available for solar zenith angles below 75 degrees, i.e. during Arctic summer.

Table S1: Zonal mean comparison of datasets using CERES and GEWEX at original resolution and Fluxnet-CLARA coarsened to approximately match them. Standard deviations not computed.

Latitude band 70 – 80 °N, June 2000-2007			
Mean difference of SRB component [W/m^2]	CERES EBAF – GEWEX SRB	CERES EBAF – Fluxnet-CLARA	GEWEX SRB – Fluxnet-CLARA
SWD	23.32	14.75	-8.57
SWU	29.19	29.49	0.30
LWD	8.08	-9.67	-17.75
LWU	6.61	-9.63	-16.24
Latitude band 80 – 90 °N, June 2000-2007			
SWD	13.50	36.79	23.29
SWU	20.51	41.90	21.39
LWD	11.27	-5.31	-16.58
LWU	19.92	6.26	-13.66

Table S2: Zonal mean comparison of datasets for July. CERES and GEWEX data resampled to 25x25 km^2 resolution.

Latitude band 70 – 80 °N, July 2000-2007			
Mean difference (Std. dev.) of SRB component [W/m^2]	CERES EBAF – GEWEX SRB	CERES EBAF – Fluxnet-CLARA	GEWEX SRB – Fluxnet-CLARA
SWD	0.60 (3.94)	-2.62 (3.19)	-3.22 (5.05)
SWU	10.89 (2.65)	16.81 (3.90)	5.92 (3.10)
LWD	5.03 (1.87)	-9.23 (1.45)	-14.26 (2.54)
LWU	-1.1 (1.13)	-14.45 (1.64)	-13.34 (1.44)
Latitude band 80 – 90 °N, July 2000-2007			
SWD	-6.98 (8.42)	30.20 (5.57)	37.18 (6.33)
SWU	-1.89 (10.73)	38.04 (7.31)	39.93 (10.25)
LWD	10.97 (2.40)	-6.68 (1.42)	-17.64 (1.52)
LWU	2.42 (2.75)	-3.84 (2.65)	-6.26 (3.04)

Table S3: Zonal mean comparison of datasets for August. CERES and GEWEX data resampled to 25x25 km^2 resolution.

Latitude band 70 – 80 °N, August 2000-2007			
Mean difference (Std. dev.) of SRB component [W/m^2]	CERES EBAF – GEWEX SRB	CERES EBAF – Fluxnet-CLARA	GEWEX SRB – Fluxnet-CLARA
SWD	-9.55 (2.14)	-6.89 (2.39)	2.66 (2.80)
SWU	3.47 (1.85)	6.10 (1.94)	2.63 (0.81)
LWD	9.65 (1.24)	-5.44 (1.84)	-15.09 (2.32)
LWU	0.00 (1.33)	-12.23 (1.97)	-12.23 (2.04)
Latitude band 80 – 90 °N, August 2000-2007			
SWD	-9.78 (6.84)	20.07 (5.07)	29.86 (5.45)
SWU	0.91 (5.21)	22.50 (5.04)	21.59 (3.81)

LWD	14.44 (2.21)	-6.01 (2.54)	-20.46 (2.50)
LWU	4.68 (3.67)	0.72 (4.65)	-3.95 (3.47)

Figure S1: Validation of CERES and Fluxnet-CLARA SWD over Tara ice camp using CERES at original resolution and coarsening Fluxnet-CLARA to match with two resampling methods.

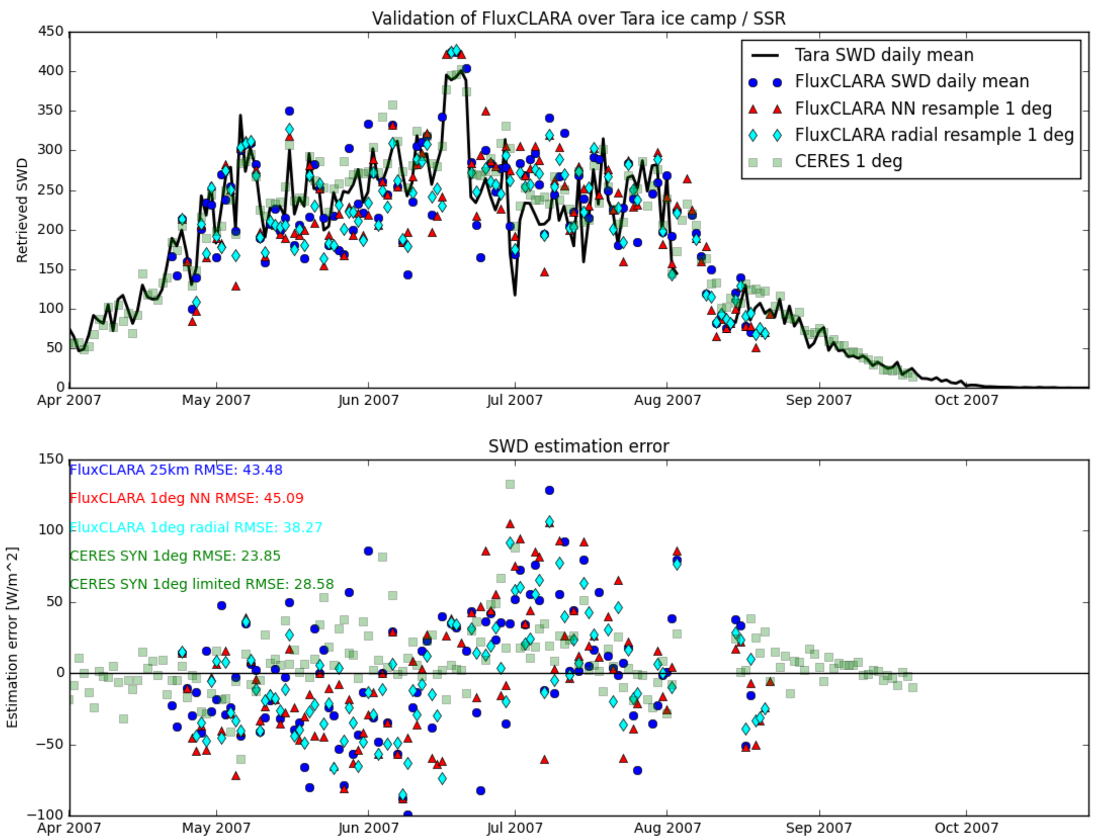

Figure S2: Validation of CERES and Fluxnet-CLARA SWU over Tara ice camp using CERES at original resolution and coarsening Fluxnet-CLARA to match with two resampling methods.

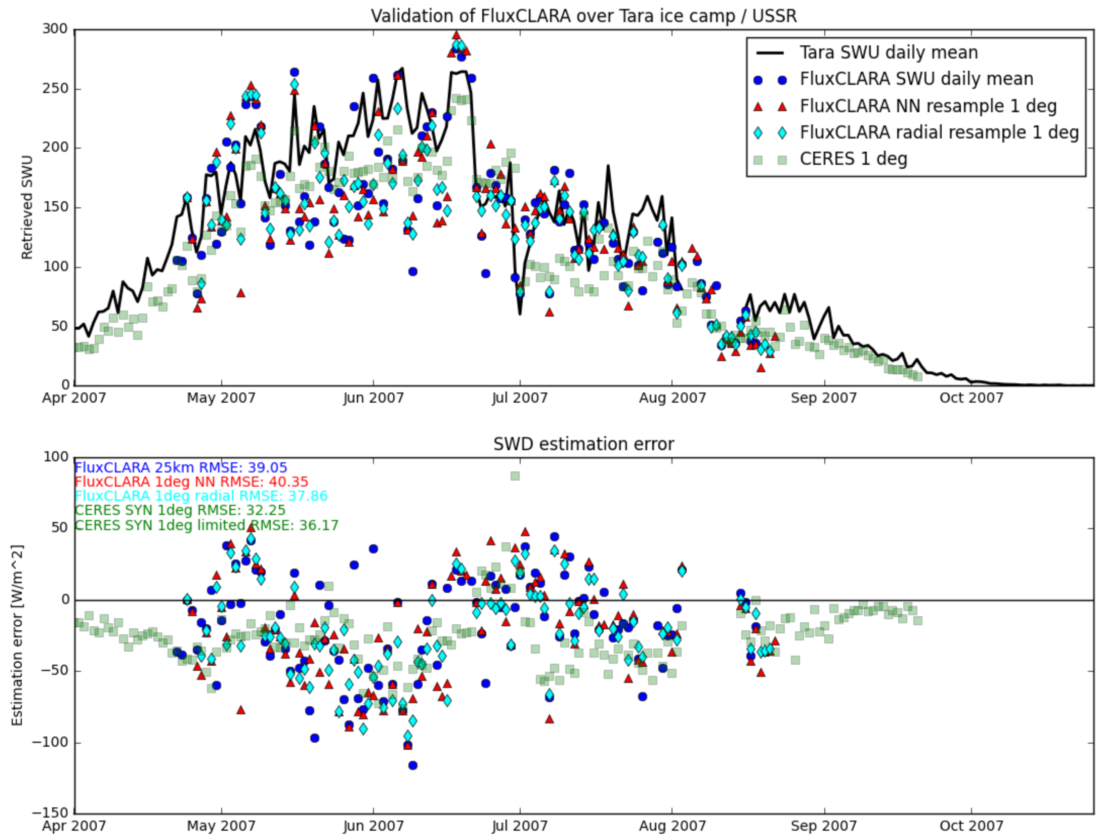

Figure S3: Validation of CERES and Fluxnet-CLARA LWD over Tara ice camp using CERES at original resolution and coarsening Fluxnet-CLARA to match with two resampling methods.

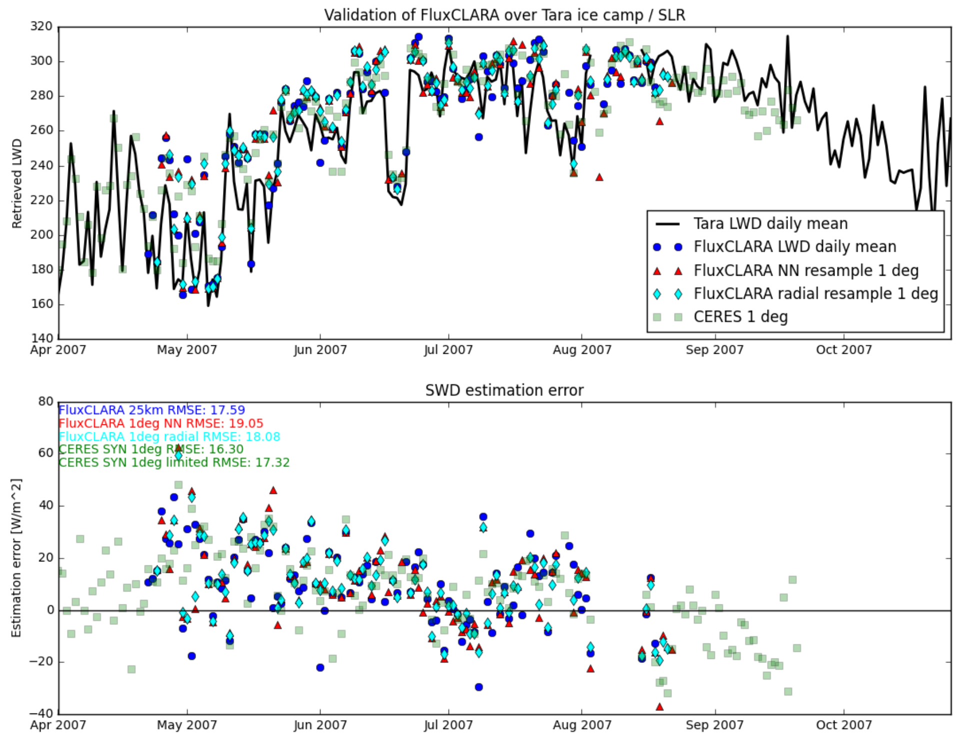

Figure S4: Validation of CERES and Fluxnet-CLARA LWU over Tara ice camp using CERES at original resolution and coarsening Fluxnet-CLARA to match with two resampling methods.

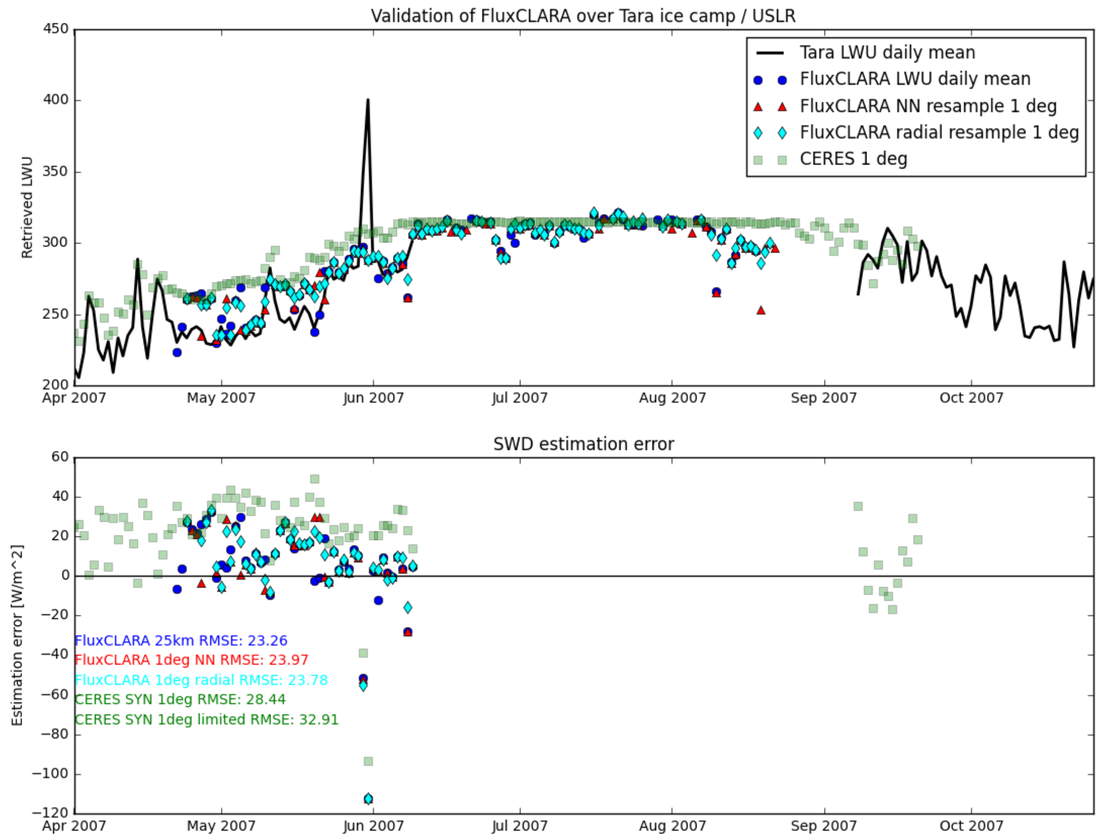

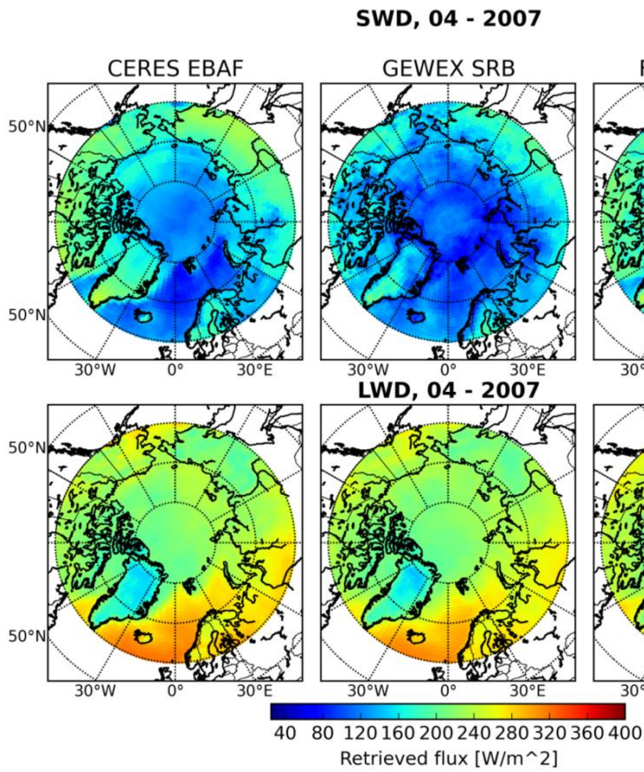

Figure S5. SWD & LWD for April 2007.

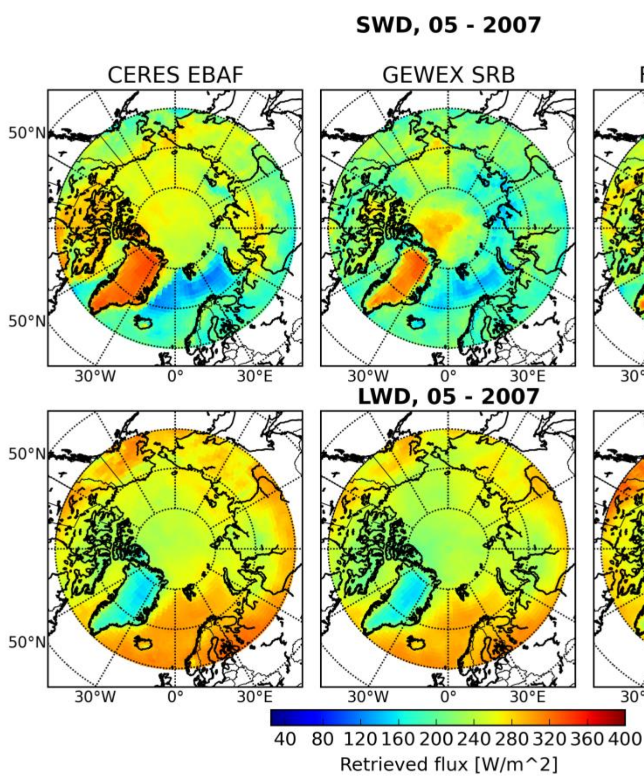

Figure S6. SWD & LWD for May 2007.

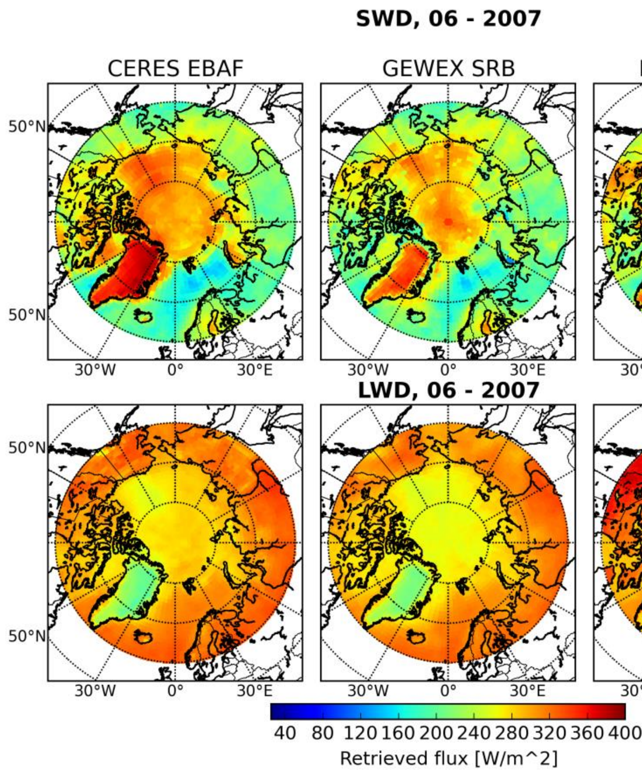

Figure S7. SWD & LWD for June 2007.

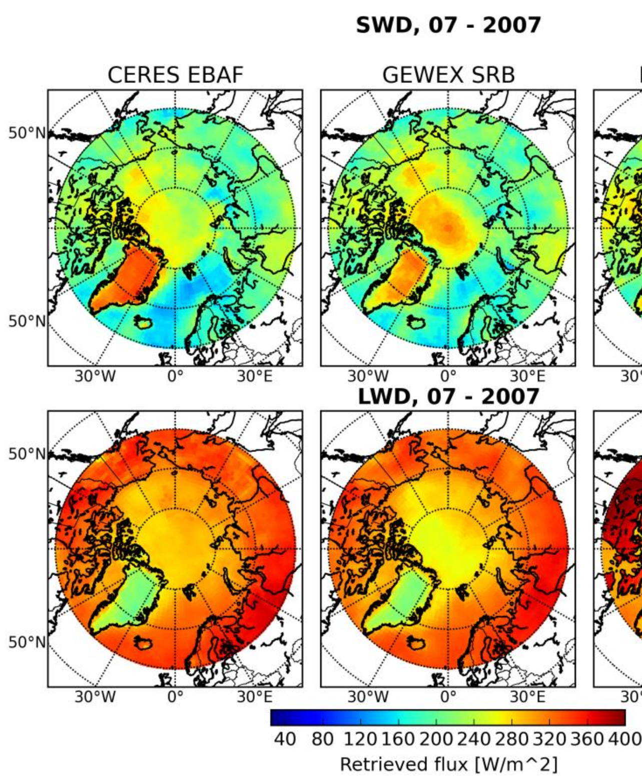

Figure S8. SWD & LWD for July 2007.

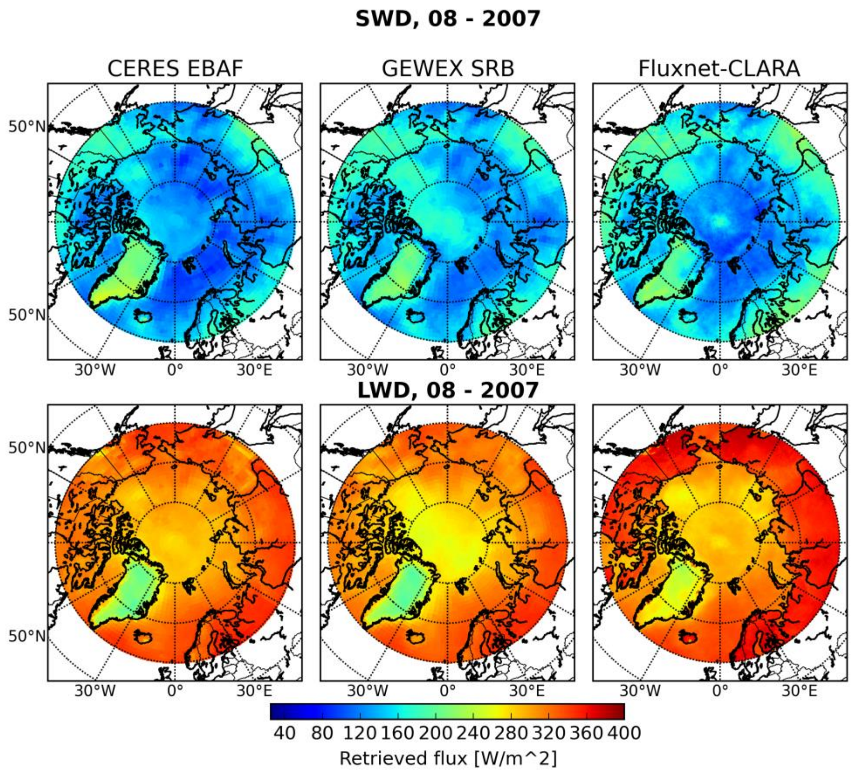

Figure S9. SWD & LWD for August 2007.

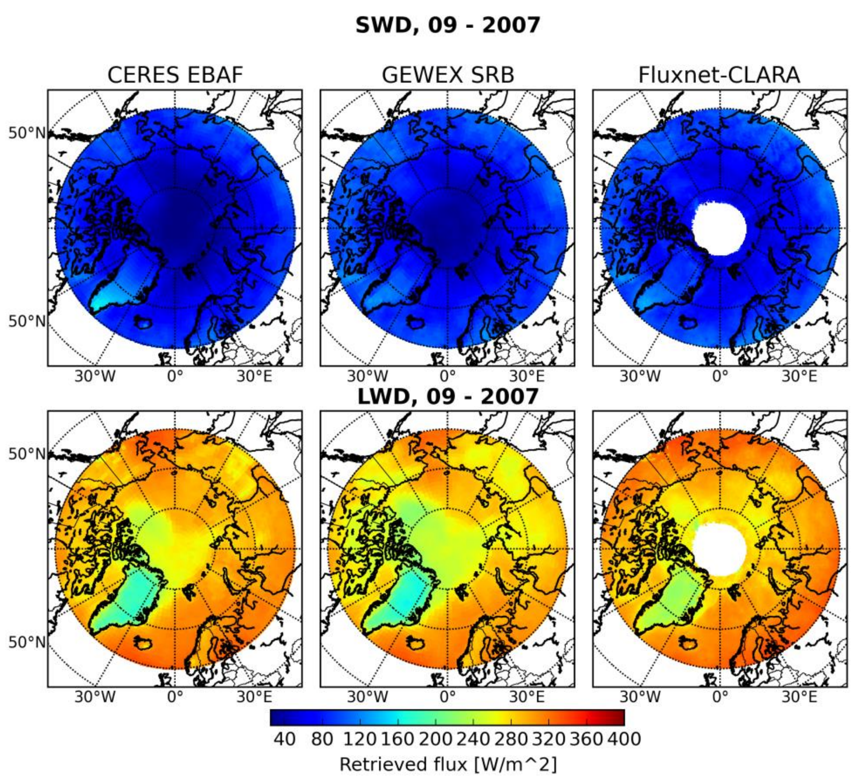

Figure S10. SWD & LWD for September 2007.

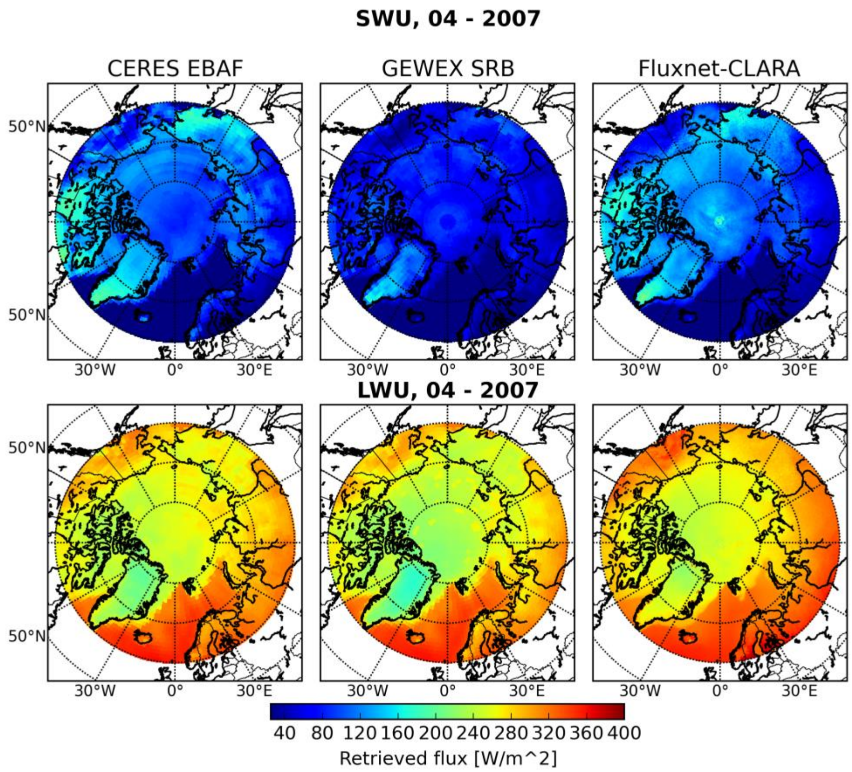

Figure S11. SWU & LWU for April 2007.

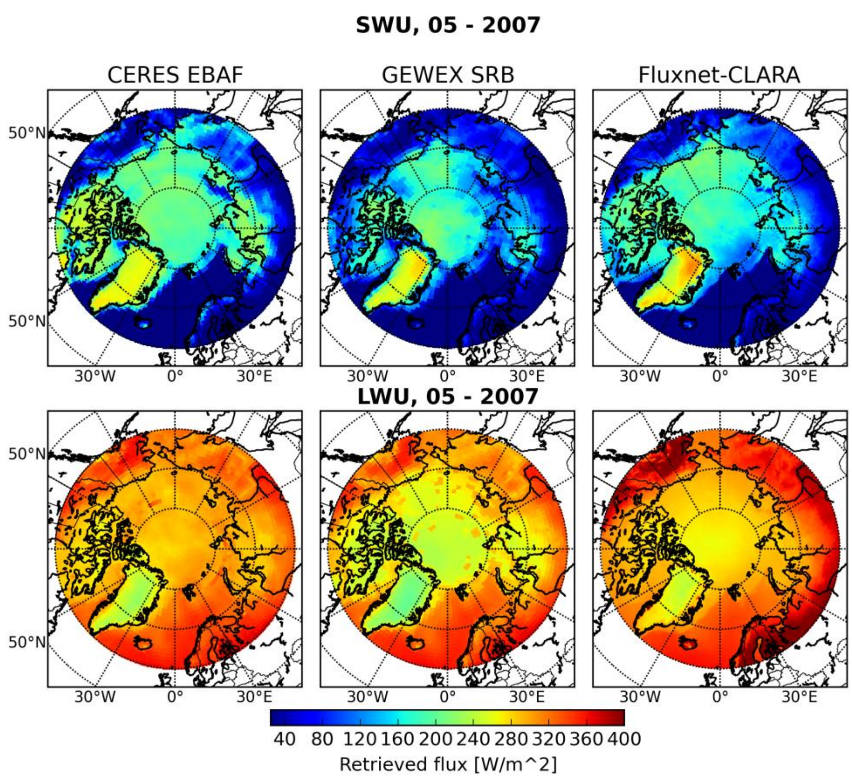

Figure S12. SWU & LWU for May 2007.

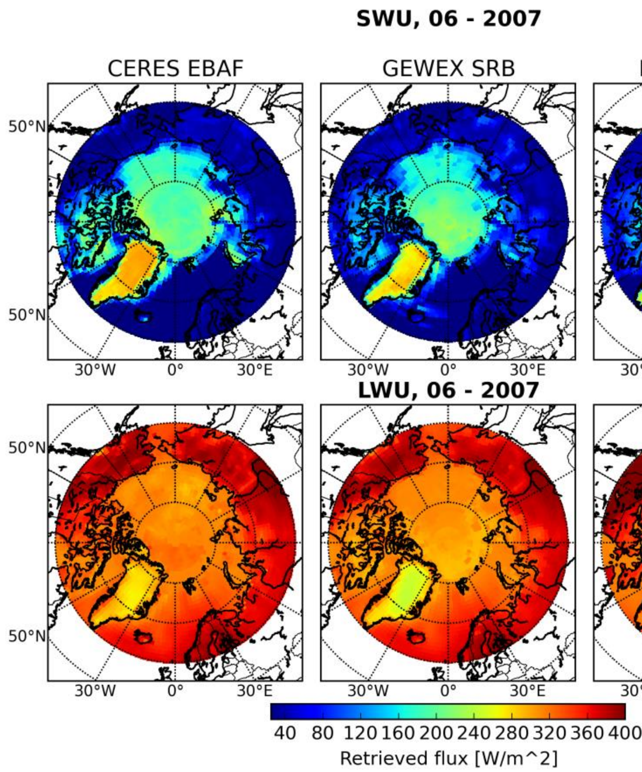

Figure S13. SWU & LWU for June 2007.

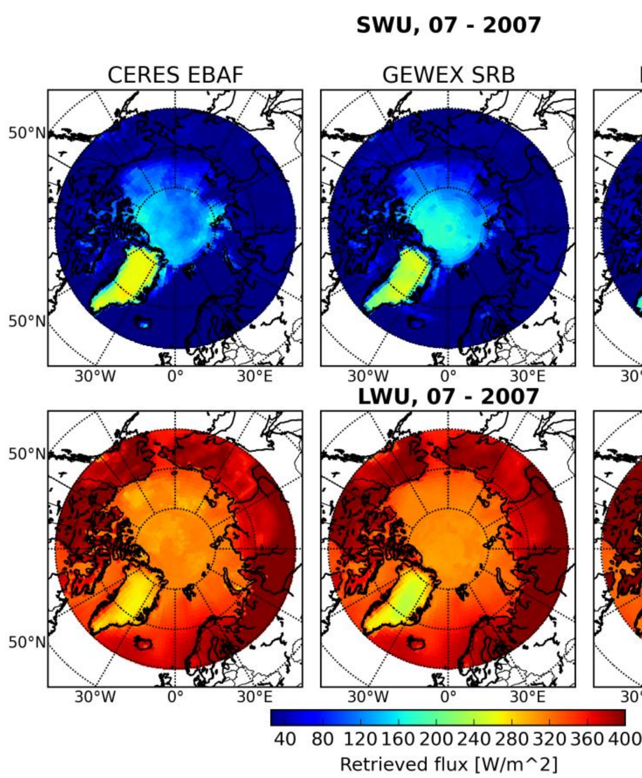

Figure S14. SWU & LWU for July 2007.

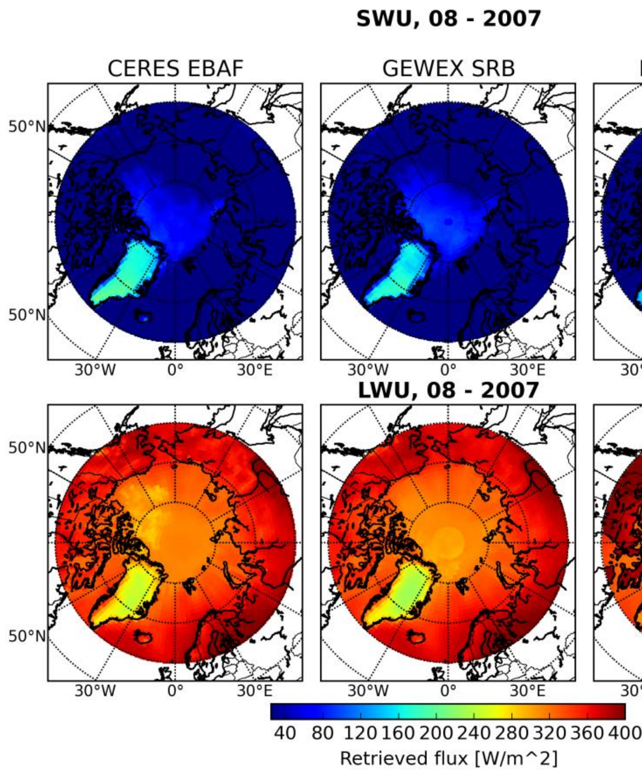

Figure S15. SWU & LWU for August 2007.

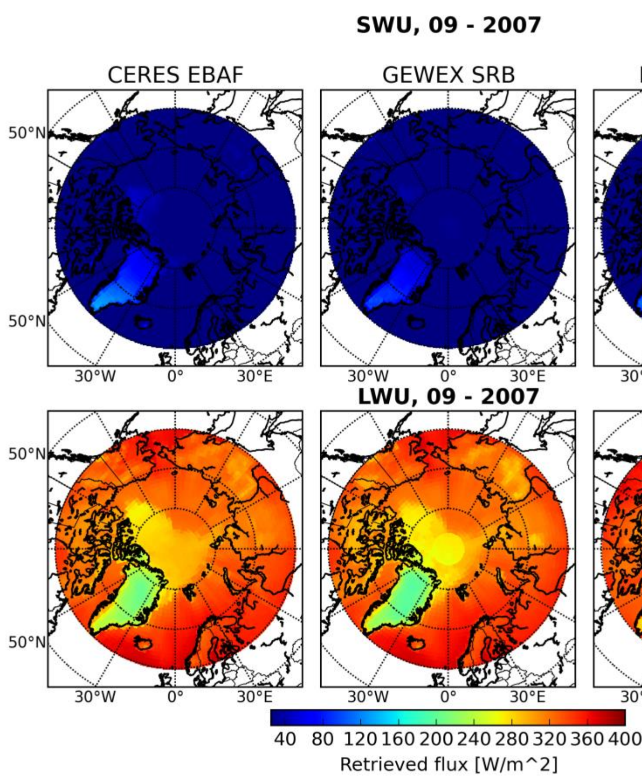

Figure S16. SWU & LWU for September 2007.